



THERMAL AND OPTICAL PROPERTIES OF SODIUM-PHOSPHO - ZINC - NEODYMIUM OXIDE GLASS SYSTEM

Asha Rajiv¹, M. Sudhakara Reddy², Jayagopal Uchil³, C. Narayana Reddy^{4*}

^{1,2,3}Department of Physics, School of Graduate Studies, Jain University, Bangalore 560027, India.

⁴Department of Physics, Sri Siddaganga college of Arts, Science and Commerce, Tumkur University, Tumkur 572103, India.

*Corresponding author: nivetejareddy@gmail.com

ABSTRACT

Neodymium doped sodium phospho-zinc oxide glasses of the composition $(80-x) \text{NaPO}_3 - 20 \text{ZnO} - x \text{Nd}_2\text{O}_3$ (where $x = 0, 0.1, 0.3, 0.5, 0.7$ mol %) have been synthesized by energy efficient microwave heating technique. In order to understand the role of neodymium in these glasses, the density, glass transition, refractive index, optical absorption and photoluminescence properties were investigated. The density and refractive index were found to increase with increasing neodymium concentration which is attributed to the formation of non-bridging oxygens (NBOs) in the glass matrices. The optical absorption spectra were measured in the wavelength range 300-1000 nm and the optical band gaps were determined. It was found that the optical band gap decreases with an increase in neodymium concentration. The photoluminescence measurements showed luminescent peaks around 880 and 1060 nm, which are due to the radiative transitions ${}^4\text{F}_{3/2} \rightarrow {}^4\text{I}_{9/2}$ and ${}^4\text{F}_{3/2} \rightarrow {}^4\text{I}_{11/2}$ of Nd^{3+} ions.

Keywords: Neodymium, Refractive index, Optical absorption, Non-bridging oxygens, Photoluminescence.

1. INTRODUCTION

In recent times, glasses doped with rare earth ions have attracted a considerable interest due to their photonic applications as optical amplifiers and solid – state lasers. Wave guide lasers and amplifiers are obtained by doping glasses with rare earth oxides [1].

Optical properties of rare- earth doped glass are found to have applications in the advancement of glass lasers as well as in the production of wide variety of optical fiber cables, prisms and commercial filter glasses. Neodymium is one of the most studied rare earth ion and is found to have immense applications in photonic devices [2, 3]. Neodymium containing glasses are used in halogen lamps to absorb ultra-violet rays, which are harmful to humans. Glasses containing neodymium have high hardness and excellent chemical durability as refractory glasses. Also these glasses can be used as a band rejection filter for image display devices, owing to absorption originating in the inter-transition within the 4f shell of the Nd^{3+} ion [4, 5]. Doping with Neodymium in the phosphate network can give a high stimulated cross-section. The well-defined and sharp energy levels of rare-earth ions serve as structural probes for the environment and the modification of the energy level structure of the rare earth ions caused by the glassy environment leads to interesting applications [6]. The application of the glasses mainly depends on the structure of the host glass and the properties of the dopant ions. The rare earth materials incorporated into the host glass gives rise to

stimulated emission which is characteristic of trivalent rare earth ions. Due to specific chemical structure and microstructural properties, zinc oxide is used in various applications and is found to be a good multifunctional material. ZnO can enter the glass network both as network former and also as a network modifier depending on the chemical composition of the glass [7]. Higher valent oxides, such as ZnO, MgO, PbO etc when used as modifiers, the cations produce important structural effects. The addition of cation to the glass network leads to the Bridging Oxygen (BO) and Non Bridging Oxygen (NBO) conversion. The increase of the NBO species in the glass matrix, leads to the general depolymerization of the network that can be related to the modifications of the chemical and physical properties [8]. With the alteration in the chemical composition of the glass, there are significant changes in the optic and spectroscopic properties and these specific properties of a laser gain material are used in designing the laser device. Extensive survey of Neodymium ion (Nd^{3+}) in silicates, phosphates, borates, sulphates, tellurites and several fluoride glasses has been reported and significant changes in spectroscopic parameters are observed. [9-12]. The glasses doped with rare-earth ions offer a variety of dopant sites with different ion-host interactions resulting in the changes occurring in spectral properties and this finds application in second generation telecommunications especially as optical amplifiers with the window at 1.3 μm . The inorganic glasses like phosphate, borate, germanate, vanadate and tellurite families are widely used for photonic applications.

Study of optical absorption and particularly the absorption edge is one of the useful methods to investigate optically induced transitions and obtain information about band structure and energy gap of both crystalline and non-crystalline materials. The optical absorption studies are used as a powerful tool for probing the local environment of a paramagnetic impurity and mapping the crystal field [13]. Photoluminescence which is actually the emission of light from a specimen under optical excitation helps in deriving much information on the emitting material and is useful in surface diagnostic as this phenomenon often originates from the surface layer of the material. In the present work, we discuss the thermal and optical properties of Neodymium doped sodium phospho-Zinc oxide glass (NPZN) system synthesized by microwave method.

2. EXPERIMENTAL

The rare earth oxide containing glasses of the system $(80-x)\text{NaPO}_3-20\text{ZnO}-x\text{Nd}_2\text{O}_3$ (where $x = 0, 0.1, 0.3, 0.5, 0.7$ mol %) were prepared by microwave heating technique using analar grade sodium hydrogen phosphate (NaHPO_4), Zinc oxide, and Neodymium oxide (Nd_2O_3) as starting materials. An appropriate quantity of weighed chemicals were mixed and thoroughly ground to homogenize the mixture and kept in a silica crucible inside a domestic microwave oven operating at 2.45 GHz and 850 W power. Within 6–8 min of microwave exposure a good homogeneous melt was obtained, which was immediately quenched between copper blocks. The silica crucible was found to remain clean and unaffected during the short duration of melting. The glass was annealed in a muffle furnace for 1 hour at 200°C to remove thermal strains that could have developed during quenching. The samples were preserved under anhydrous Calcium chloride atmosphere (CaCl_2). The density of the glasses was measured by the Archimedes principle using toluene ($\rho_{\text{Toluene}} = 0.860 \text{ gm/cc}$) as the immersion liquid. The molar volume (M_v) was calculated using $M_v = M/\rho$, where M is the molecular weight. The accuracy of weight determination was ± 1 milligram. Glass transition (T_g) of the samples were recorded using Differential Scanning Colorimeter (Perkin Elmer DSC-2). The accuracy in the measurements of T_g was ± 2 K. UV-Visible Absorption spectra of synthesized glasses was recorded using Perkin Elmer (Lambda 35) spectrometer in the UV-Vis-NIR region in the range 300 to 900 nm. Refractive indices of these glasses have been measured in the wavelength 589.3 nm at 30°C using Digital Abbe Refractometer (DR-A1) with Methylene Iodide containing Sulphur solution as the contact layer between the sample and prism of the refractometer by using sodium vapor lamp as the light source. Absorbance of glasses were measured using USB4000 Fiber Optic Spectrometer that was connected to a computer and controlled by SpectraSuite software. The UV-light was transmitted through the optical fiber to the sample. The spectrometer measured the amount of light and

transformed it into digital information and passed the sample information to SpectraSuite which compared the sample to the reference measurement and displayed processed spectral information.

Photoluminescence emission spectra of glasses doped with different concentrations of Nd_2O_3 were recorded at 325nm excitation wavelength at room temperature using a LabRAM HR (UV) system, which has high spectroscopic resolution and a unique wavelength range capability.

3. RESULTS AND DISCUSSION

3.1. Density and Molar volume

Density is composition dependent and can play a key role for the optical and volume measurements of amorphous materials. Density variations can change some optical properties of glass. The variations of density and molar volume for neodymium doped sodium phospho-zinc oxide glass samples are shown in Fig. 1. It can be seen from Fig. 1, that density increases while molar volume decreases when Nd_2O_3 composition in the glass samples varies from 0 to 0.7 mol %. This may be due to the fact that addition of Nd_2O_3 modifies the NaPO_3 glass network, leading to greater connectivity and compactness of the glass structure. It is evident from Fig.1, that density is dominated by the Nd_2O_3 content and increases as Nd_2O_3 replaces NaPO_3 constituents. Further, the molar volume was observed to vary between 42.925 to 33.373 cc and depends primarily on the presence of phosphate units in the network structure of glass. In the investigated glasses ZnO is being kept constant at 20 mol% and NaPO_3 is replaced by heavier Nd_2O_3 . The increase in density is due to the high relative molecular mass of Nd_2O_3 (336.48 g/mol) compared to NaPO_3 (101.96 g/mol).

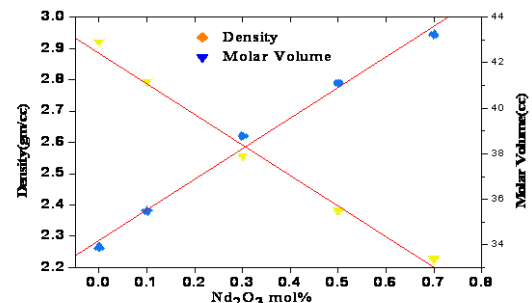


Fig. 1: Variation of Density and Molar volume with Nd_2O_3 mol %

The concentration of the rare-earth ions is an important parameter as it affects the laser gain of the host material and the physical properties provide an insight into the atomic arrangements. The various physical parameters like neodymium ion concentration (N), polaron radius (r_p), inter-nuclear distance (r_i) and field strength (F) can be determined

from the density, average molecular weight and concentration of the rare-earth ions, using the standard relations (1-4). All the above mentioned physical properties are listed in Table 1.

$$N \text{ (ion/cm}^3\text{)} = \frac{(\% \text{ mol of Nd}_2\text{O}_3) \times (\text{Avogadro's number} \times \text{glass density})}{(\text{glass average molecular weight})} \quad (1)$$

$$\text{Polaron radius, } r_p \text{ (\AA)} = \frac{1}{2} \left(\frac{\pi}{6N} \right)^{1/3} \quad (2)$$

$$\text{Inter nuclear distance, } r_i \text{ (\AA)} = \left(\frac{1}{N} \right)^{1/3} \quad (3)$$

$$\text{Field strength, } F \text{ (cm}^{-2}\text{)} = \left(\frac{Z}{r_p^3} \right) \quad (4)$$

It is noticed that the total neodymium concentration N increases where as the polaron radius and internuclear distance of rare earth ions are found to decrease with the increase in neodymium oxide content in the compositions. The increase in density observed is attributed to increase in the rigidity of glass and increase in field strength tends to attract the oxygen ions, leading to a decrease in the size of the interstices.

Table 1: Concentration of Neodymium ions (N) in 10^{20} ions/cc, Polaron radius (r_p) in Å, Inter ionic distance (r_i) in Å and field strength (F) in 10^{15} cm^{-2} of neodymium doped sodium phospho-zinc oxide glass system

Sample Code	N	r_p	r_i	F
NZN0	-----	----	-----	-----
NZN1	0.1462	3.584	8.895	2.335
NZN2	0.4802	1.631	5.927	11.277
NZN3	0.8483	1.349	4.903	16.485
NZN4	1.2457	1.180	4.314	21.328

3.2. Glass transition temperature

Glass transition temperature (T_g) plays a vital role in maintaining thermal and mechanical properties of glasses. Fig. 2 shows the DSC thermograms. T_g values are extracted from the thermograms. It is the point corresponding to the intersection of the linearly extended arms of the rising part of the endothermic elbow. Fig. 3 shows the variation of glass transition temperature with Neodymium composition. As can be seen from Fig. 3, T_g increases (from 501 K to 568 K) monotonically with the increase in concentration of Nd_2O_3 . This indicates the greater connectivity and rigidity in the network because of the increase of the cross-linking which can be attributed to the neodymium ions in the interestials.

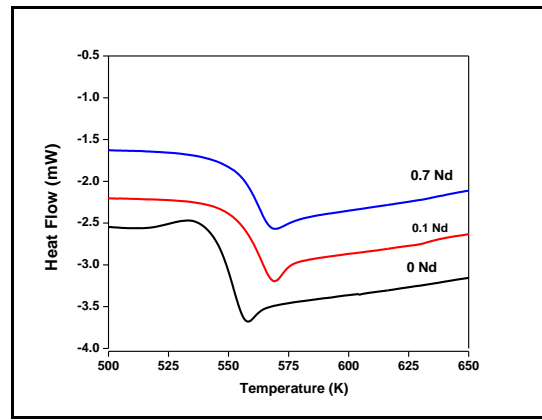


Fig.2. DSC thermograms of neodymium doped glass system

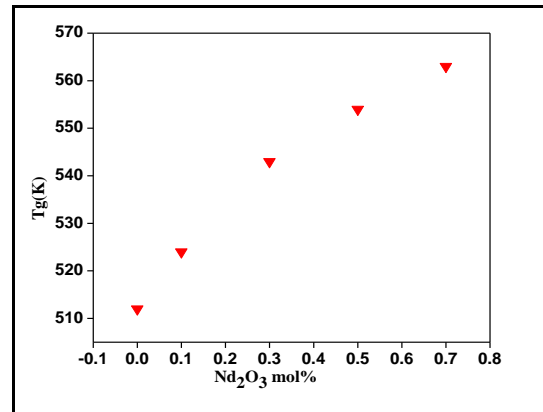


Fig. 3: Variation of T_g with Nd_2O_3 mol%

3.3. Optical absorption spectra

The optical absorption spectrum of Nd^{3+} doped glasses is shown in Fig. 4. It is observed that the absorption intensity of the observed bands increases with the increase of Nd_2O_3 concentration. The absorption coefficient values corresponding to the absorption bands are dependent on neodymium oxide concentration. The transition ${}^4I_{9/2} \rightarrow {}^4F_{5/2} + {}^2H_{9/2}, {}^4F_{7/2} + {}^4S_{3/2}, {}^2G_{7/2} + {}^4G_{5/2}, {}^2K_{13/2} + {}^4G_{7/2} + {}^4G_{9/2}, {}^4D_{3/2} + {}^4I_{11/2} + {}^4D_{5/2}, {}^4D_{1/2} + {}^2L_{15/2}$ between the ground state and higher energy states inside the $4f^3$ electronic configuration of the Nd^{3+} ions are observed in the 400-900 nm spectral region. The assignments of these transitions are made on the basis of Carnell *et al* [14]. The absorption coefficient, $\alpha(\nu)$ [15] has been calculated for each sample at different phonon energies using the relation (5).

$$\alpha(\nu) = \left(\frac{1}{d} \right) \ln \left(\frac{I_0}{I_t} \right) \quad (5)$$

Where, ' I_0 ' and ' I_t ' are intensities of the incident and transmitted beams and ' d ' corresponds to thickness of sample. The extinction coefficient (K) has been calculated using the relation

$$K = \frac{\alpha \lambda}{4\pi} \quad (6)$$

The experimental oscillator strength (f_{meas}) of the absorption transitions [16] for determining the intensity of the transitions has been calculated using relation (7) are listed in Table 2.

$$f_{meas} = 4.32 \times 10^{-9} \int_{\nu_1}^{\nu_2} \epsilon(\nu) d\nu \quad (7)$$

Where $\epsilon(\nu) = OD/ct$ is the molar extinction coefficient, 'OD' the optical density, 'c' the concentration in moles/lit and 't' the optical length of the glass in cm.

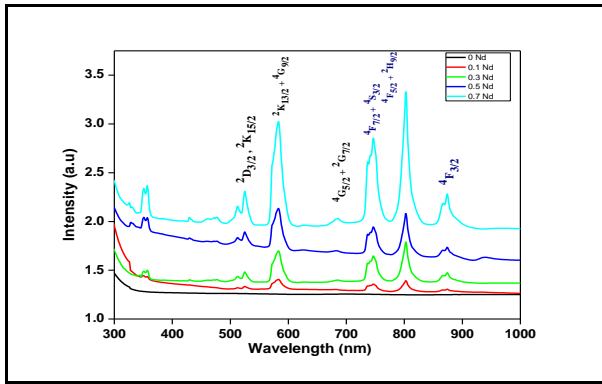


Fig.4. Optical absorption spectra of Nd³⁺ doped glasses

Table 2: Theoretically calculated energy levels (cm⁻¹) and experimentally measured oscillator strength for various concentrations of Nd³⁺ ions in sodium phospho- zinc oxide glasses

Glass	Transition	Assignment	λ (nm)	Energy (cm ⁻¹)	Oscillator strength f_{meas} (10 ⁻⁶)
NZN1	⁴ I _{9/2}	⁴ F _{5/2} + ² H _{9/2}	802	12,468	13.725
		⁴ F _{7/2} + ⁴ S _{3/2}	747	13,386	11.759
		² G _{7/2} + ⁴ G _{5/2}	583	17,152	5.983
		² K _{13/2} + ⁴ G _{7/2} + ⁴ G _{9/2}	525	19,047	7.684
		⁴ D _{3/2} + ⁴ I _{11/2} + ⁴ D _{5/2} + ⁴ D _{1/2} + ² L _{15/2}	350	28,571	4.020
NZN2	⁴ I _{9/2}	⁴ F _{5/2} + ² H _{9/2}	803	12,453	9.420
		⁴ F _{7/2} + ⁴ S _{3/2}	746	13,404	7.985
		² G _{7/2} + ⁴ G _{5/2}	583	17,152	7.196
		² K _{13/2} + ⁴ G _{7/2} + ⁴ G _{9/2}	525	19047	5.583
		⁴ D _{3/2} + ⁴ I _{11/2} + ⁴ D _{5/2} + ⁴ D _{1/2} + ² L _{15/2}	351	28,490	4.447
NZN3	⁴ I _{9/2}	⁴ F _{5/2} + ² H _{9/2}	805	12,422	151.3
		⁴ F _{7/2} + ⁴ S _{3/2}	748	13,368	120
		² G _{7/2} + ⁴ G _{5/2}	585	17,094	92.03
		² K _{13/2} + ⁴ G _{7/2} + ⁴ G _{9/2}	526	19,011	41.07
		⁴ D _{3/2} + ⁴ I _{11/2} + ⁴ D _{5/2} + ⁴ D _{1/2} + ² L _{15/2}	358	27,932	36.8
NZN4	⁴ I _{9/2}	⁴ F _{5/2} + ² H _{9/2}	803	12,453	91.27
		⁴ F _{7/2} + ⁴ S _{3/2}	747	13,386	58.6
		² G _{7/2} + ⁴ G _{5/2}	583	17,152	51.118
		² K _{13/2} + ⁴ G _{7/2} + ⁴ G _{9/2}	525	19,047	17.377
		⁴ D _{3/2} + ⁴ I _{11/2} + ⁴ D _{5/2} + ⁴ D _{1/2} + ² L _{15/2}	357	28,011	24.07

With the doping of rare earth oxides, a shift in wavelength is observed and this effect is called nephelauxetic effect [17]. This happens due to the deformation of the electronic orbitals within the 4f configuration. With the increase in the overlap of 4f and oxygen orbitals, the energy level structure of Nd³⁺ ion contracts, leading to shift in the wavelength. A shift in the wavelength towards higher side is observed for almost all the transitions which is an indication of the presence of Nd - O linkages in the glass system. The transitions ⁴I_{9/2} → ⁴F_{5/2} + ²H_{9/2} is found to be more intense than the other transitions which is very well seen from the intensity of the experimentally calculated oscillator strengths.

Direct and indirect optical band gaps were calculated using Davis and Mott [18] equation (8) which correlates absorption coefficient $\alpha(\nu)$ as a function of photon frequency ($h\nu$)

$$\alpha(\nu) = B(h\nu - E_{opt})^n/h\nu \quad (8)$$

Where, the exponent $n= 1/2$ for an allowed direct transition, $n= 2$ for an allowed indirect transition and ‘B’ is a constant. The optical energy band gap (E_{opt}) for indirect and direct transitions were found, by plotting $(\alpha hv)^{1/2}$ and $(\alpha hv)^2$ as a function of photon energy (Tauc’s plot). The Tauc’s plots for the glass samples are shown in Fig. 5 and Fig.6. By plotting $(\alpha hv)^{1/2}$ and $(\alpha hv)^2$ as a function of photon energy hv , optical band gaps for indirect and direct transitions were found. The respective values of E_{opt} were obtained by extrapolating to $(\alpha hv)^{1/2}=0$ for indirect transitions and $(\alpha hv)^2= 0$ for direct transitions [19].

It can be seen that there exists a linear dependence of $(\alpha hv)^{1/2}$ in the photon energy. This suggests that at higher photon energies the transitions occurring in the present glass samples are of indirect type. The obtained values of the optical band gap are listed in Table 3. It can be noted that the optical band gap energy (E_{opt}) decreases and the Urbach energy (ΔE) increases with the increase in concentration of neodymium ions which can be probably related to the progressive increase in the concentration of NBOs [20]. The introduction of rare earth oxide into the sodium phospho - zinc oxide network increases the non-bridging oxygen concentration and thus creates different oxidation states due to the mixed ions in the form of oxygen bridged. This could be the reason why the absorption edge has shifted towards the higher energy which leads to the decrease in the optical gap.

Table 3: Thickness (d), direct and indirect optical band gaps and Urbach energies of glass samples

Glass code	d (mm)	E_{opt} (direct) (eV)	E_{opt} (indirect) (eV)	ΔE_0 (eV)
NZN0	1.777	4.283	3.241	0.553
NZN1	1.306	4.167	3.236	0.578
NZN2	1.545	4.150	3.153	0.607
NZN3	1.278	4.098	3.056	0.624
NZN4	1.407	3.914	2.962	0.668

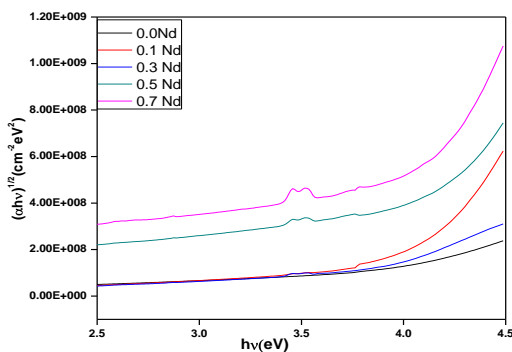


Fig. 5: Plots corresponding to indirect band gap for Nd³⁺ doped glass

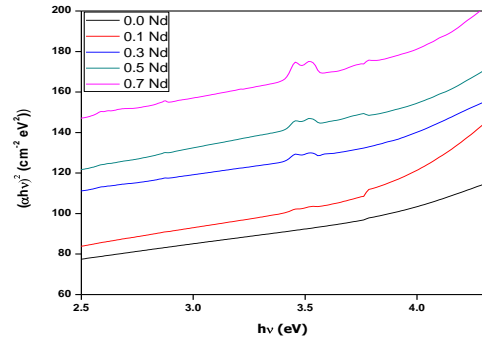


Fig. 6: Plots corresponding to direct band gap for Nd³⁺ doped glass

Refractive index is one of the optical parameters that finds importance in lasing action of optical materials. Therefore, many investigators carried out investigations to ascertain the correlation between refractive index and composition of glass. The determination of refractive index is essentially important in correlating the theory of electronic structure and properties of amorphous materials. The refractive index of the Nd³⁺ doped glasses measured using Digital Abbe Refractometer (DR-AI) is given in Table 4. The increment in the refractive index leads to an increase in density and dielectric constant. The dielectric constant (ϵ) was calculated from the refractive index of the glass using the relation (9).

$$\epsilon = n_d^2 \tag{9}$$

The reflection loss from the glass surface was computed from the refractive index by using the Fresnel’s formula [10]

$$R = \left[\frac{(n_d - 1)}{(n_d + 1)} \right]^2 \tag{10}$$

The value of molar refraction (R_M) was calculated using the relation (11) given by Duffy and Ingram [25].

$$\frac{n_d^2 - 1}{n_d^2 + 2} \left(\frac{M}{\rho} \right) = R_M \tag{11}$$

The molar refraction also shows a consistent increase and is found to depend on the refractive index, density and average molecular weight of glass and is consistent with all the physical parameters determined. The values of reflection loss and molar refraction are listed in Table 4. Electronic polarizability of an ion is related to properties of the material such as refraction, conductivity, optical nonlinearity along with optical basicity and is of significant interest to study the polarization state of ions in crystalline and amorphous materials [21]. Molar refraction is related to the structure of the glass and it is proportional to the molar electronic polarizability of the material, through the Clausius–Mossotti relation [22].

$$\alpha_M = \left(\frac{3}{4\pi N} \right) R_M \tag{12}$$

Where N is the number of polarizable ions per mole and is assumed to be equal to the Avogadro’s number (N_A). The value

$4\pi/3$ is known as a constant in Lorentz function. With α_m in (10^{-24}cm^3) , [12] can be transformed to $R_m = 2.52 \alpha_m$.

The average electronic polarizability of oxide ions in multicomponent oxide glasses were calculated using the relation (13) given by Chimalawong et al [22]

$$\alpha_0^{2-}(n) = \left[\frac{R_m}{2.52} - \sum \alpha_{cat} \right] / N_0^{2-} \quad (13)$$

Where, $\sum \alpha_{cat}$ denotes the molar cationic polarizability and N_0^{2-} the number of cation ions in the multicomponent oxide glasses. The molar cation polarizability of the glasses can be calculated using the data of polarizability of cations having the following values: $\text{Na}^+ = 0.181 \text{ \AA}^3$, $\text{P}^{5+} = 0.021 \text{ \AA}^3$, $\text{Nd}^{3+} = 2.546 \text{ \AA}^3$ and $\text{Zn}^{2+} = 0.283 \text{ \AA}^3$ [23]. The various optical parameters discussed above are listed in Table 4. It can be seen that the oxide ion polarizability increases linearly with increase of refractive index. The results show that the refractive index of glass not only depends on the density but also on the electronic polarizability of the glass [24, 25]. This agrees with the results of Dimitrov [21] that there is a general trend of an increase of oxide ion polarizability with increasing refractive index and decreasing energy gap.

Duffy and Ingram [26] reported that the optical basicity of an oxide glass reflects the ability of the glass to donate negative charges to the probe ion and were estimated using the relation (14).

$$\Lambda_{\tau h} = \sum_{i=1}^n \frac{Z_i r_i}{2v_i} \quad (14)$$

Where, 'n' is the total number of cations present, 'Z' is the oxidation number of the i^{th} cations, 'r_i' is the ratio of i^{th} cations to the number of oxides present and 'v_i' is the basicity moderating parameter of the i^{th} cation. The basicity moderating parameter v_i was calculated using the relation (15) put forth by Duffy and Ingram [26].

$$v_i = 1.36 (X_i - 0.26) \quad (15)$$

Where, 'X_i' is the Pauling electronegativity [Pauling 1960] of the cation.

It is observed that the optical basicity values of the glasses are increasing with Nd₂O₃ content change. The optical basicity evaluated for the glasses increases when NaPO₃ is replaced by neodymium oxide. The increase of optical basicity means to increase the ability of oxide ions to transfer electrons to the surrounding cations. An increase in optical basicity indicates decrease in covalency. The increasing trend of optical basicity and oxide polarizability is in agreement with the conclusions made by Duffy [27, 28].

Table 4: Refractive index (n_D), dielectric constant (ε), molar refractivity (R_m) in cm³, molar electronic polarizability (α_m) in Å³, glass oxide polarizability (α₀²⁻) in Å³ and optical basicity (Λ_{τh}) of NPZN glasses.

Sample code	n _D	ε	R _m	α _m	α ₀ ²⁻	Λ _{τh}
NZN0	1.65	2.722	15.696	6.227	2.331	0.5031
NZN1	1.72	2.958	16.269	6.455	2.397	0.5042
NZN2	1.75	3.062	16.577	6.578	2.443	0.5062
NZN3	1.80	3.240	17.276	6.855	2.548	0.5082
NZN4	1.87	3.496	18.156	7.204	2.680	0.5102

3.4. Photoluminescence

Neodymium has been investigated as potential candidate for 1.3μm amplifier in a variety of glass doping since Nd³⁺ has emission band near 1.3μm. Neodymium which is a part of the lanthanide series in the periodic table of the elements, has the the ground-state electronic configuration as [Xe] 4f⁴ 6s₂. Ionized state of Nd³⁺ has both the 6s₂ electrons and one 4f electron missing. All the shells, except 4f-shell, are filled and thus have no contribution to the total orbital and spin momentum. Luminescent transitions within the 4f-shell can occur due to mixing with allowed transitions. Such metastable states in which the electrons reside, give rise to long luminescent lifetimes and low absorption coefficients. The photoluminescence of Nd³⁺ is ascribed to the 4f₂5d₁-4f₃ transition from the excited state to the ground state [29]. However, the photoluminescent emission of the above transitions depends significantly on the host materials. Fig.7 shows the energy level transitions in neodymium.

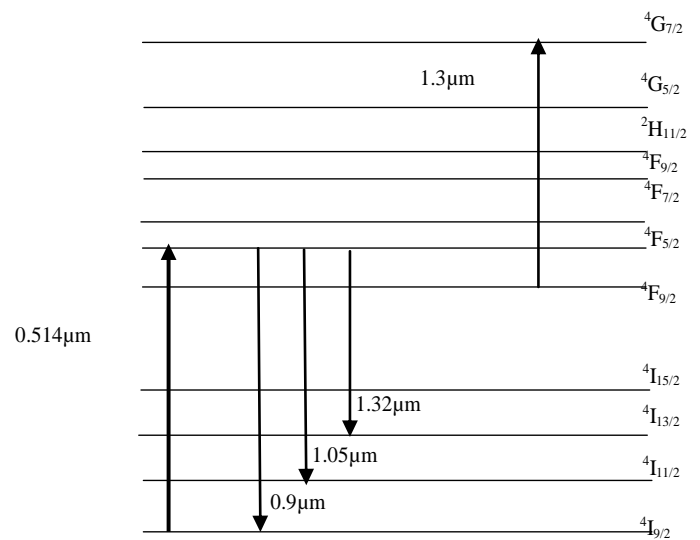


Fig. 7: Energy levels of Nd³⁺ ion

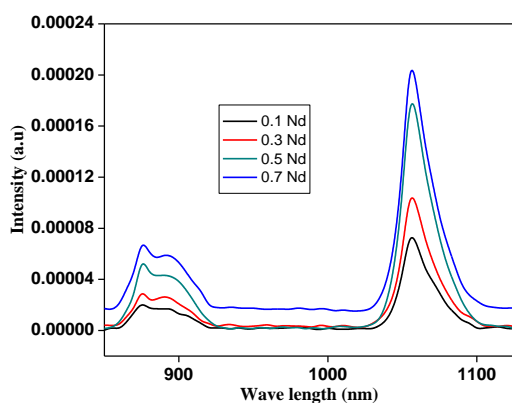


Fig. 8: PL of Nd doped glass system

The emission spectra of the glasses are shown in Fig. 8. The output of a laser at 514 nm, which is at resonance with the ${}^4F_{5/2} + {}^2H_{9/2}$ absorption line of neodymium ion, was used to pump the metastable level of ${}^4F_{3/2}$. From the spectra two luminescent peaks are found around 880 and 1060 nm which is due to the radiative transitions ${}^4F_{3/2} \rightarrow {}^4I_{9/2}$ and ${}^4F_{3/2} \rightarrow {}^4I_{11/2}$ of Nd^{3+} ions. The peak intensities increases with increase in concentration of Nd_2O_3 . The absorption and luminescent spectra are wider, which are the characteristic of amorphous materials. Among the two transitions ${}^4F_{3/2} \rightarrow {}^4I_{11/2}$ will be the potential lasing transition because of its higher stimulated emission cross-section. Neodymium doped glasses as amplifiers and lasers at 1060 nm have been widely studied and reported in both bulk materials as well as waveguide structures [30 -32]. Furthermore, the emission on the ${}^4F_{3/2} \rightarrow {}^4I_{9/2}$ ground-state transition around 865-930 nm is of interest for signal amplification in integrated optical applications, e.g. data transmission in optical interconnects and medical diagnostics. However, the efficiency at this wavelength range is not as large as that of the ${}^4F_{3/2} \rightarrow {}^4I_{11/2}$ due to the re-absorption by Nd^{3+} ions in their ground state.

4. CONCLUSION

In the present study Neodymium doped sodium phosphor-Zinc oxide glasses were prepared by novel energy efficient microwave method. The density and glass transition is found to increase with increasing concentration of Nd_2O_3 . This is due to the depolymerisation of the glass network and results in the formation of non-bridging oxygens. The decrease in optical band gap with the increase in Nd_2O_3 content is attributed to the structural changes and the absorption edge is found to shift towards the longer wavelength. The electronic polarizability and optical basicity increases with the increasing Nd_2O_3 concentration, which is in agreement with the decrease of optical band gap. The results found had illustrated the correlation of the refractive index to the density and electronic polarizability of the glass. The optical studies showed that these glasses are suitable as laser materials. The structural and

absorption properties helped in understanding the radiative and non-radiative phenomena. The luminescence spectra had transitions in the range of ${}^4F_{3/2} \rightarrow {}^4I_{9/2}$ and ${}^4F_{3/2} \rightarrow {}^4I_{11/2}$ which makes it suitable for lasing applications.

5. REFERENCES

1. Chowdari BVR, Gopalakrishnan R, Goh S.H, Tan KI. *J. Mater. Sci*, 1998; **23**:1248-1254.
2. Gatterer K, Pucker G, Jantscher W, Fritzer H.P, Arafa S. *J. Non-Cryst. Solids*, 1998; **231**:189-199.
3. Maumita Das, Annapurna K, Kundu P, Dwivedi RN, Buddhudu S. *Materials Letters*, 2006; **60**:222-229.
4. Shaweta Mohana, Kulwant Singh Thind, Gopi Sharma, Leif Gerward. *Spectrochimica Acta Part A*, 2008; **70**:1173-1179.
5. Moorthy LR, Rao TS, Jayasimhadri M, Radhapaty A, Murthy DVR. *Spectrochimica Acta Part A*, 2004; **60**:2449-2458.
6. Pisarski WA, Goryczka T, Wodecka-Dus B, Plonska M, Pisarska J. *Materials Science and Engineering B*, 2005; **122**:94-99.
7. Ganguli M, Harish Bhat M, Rao KJ. *Mater. Res. Bull.*, 1999; **34(10-11)**:1757-1772.
8. Bonamartini CA, Cannillo V, Montorsi M, Siligardi C, Cormack AN. *J. Non-Crystal. Solids*, 2005; **351**:1185-1191.
9. Marion JE, Weber MJ. *Eur. J. Solid State Inorg. Chem.*, 1991; **28**: 271-287.
10. Nageno Y, Takebe H, Morinaga K. *J. Am. Ceram. Soc.*, 1993; **76(12)**:3081-3086.
11. Batyaev IM, Golodova IV. *Optics and Spectroscopy*, 1995; **78(3)**:421-423.
12. Pozza G, Ajo D, Bettinelli M, Speghini A, Casarin M. *Solid State Commun*. 1996; **97(6)**:521-525.
13. Exarhos GJ, Risen Jr WM. *Solid State Commun*, 1972; **11**:755-758.
14. Carnall WT, Fields PR, Rajnak K. *J. Chem. Phys*, 1968; **49(10)**: 4424-4442.
15. Sindhu S, Sanghi S, Agarwal A, Seth VP, Kishore N. *Mate. Chem. Phys.*, 2005; **90**:83-89.
16. Reisfeld R, Lieblich N. *J. Phys. Chem. Solids*, 1973; **34(9)**:1467-1476
17. Naftaly M, Jha A. *Journal of Applied Physics*, 2000; **87**:2098-2104.
18. Mott NF, Davis EA. "Electronic Processes in Non-Crystalline Materials", Clarendon Press: Oxford Univ. Press, Oxford; 1971, pp. 437.
19. Chakradhar RPS, Ramesh KP, Rao J L, Ramakrishna J. *J. Phys. Chem. Solids*, 2003; **64**:641-650.
20. Bendow B, Benerjee PK, Drexhage MG, Lucas J. *J. Am. Ceram. Soc.*, 1985; **68(4)**:C92-C95.
21. Dimitrov V, Komatsu T. *Journal of Solid State Chemistry*, 2002; **163(1)**:100-112.
22. Chimalawong P, Kaewkhao J, Kedkaew C, Limsuwan P. *J. Physics and Chemistry of Solids*, 2010; **71**:965-970
23. Xinyu Zhao, Xiaoli Wang, Hai Lin, Zhiqiang Wang. *Physica B*, 2007; **392**:132-136.
24. Abdel-Baki M, Abdel-Wahab FA, Radi A, El-Diasty F. *J. Physics and Chemistry of Solids*, 2007; **68(8)**:1457-1470,
25. Abdel-Baki M, El-Diasty F, Wahab FAA. *Optics Communications*, 2006; **261(1)**:65-70.
26. Duffy JA, Ingram MD. *J. Inorg. Nucl. Chem.*, 1975; **37**:1203-1206.

27. Duffy JA, Ingram MD. *J. Non-Cryst. Solids*, 1976; **21(3)**:373-410
28. Duffy JA, Ingram MD. *J. Amer. Ceram. Soc.*, 1971; **93**:6448-6454.
29. Peijzel PS, Vergeer P, Meijerink A, Reid MF, Boatner L, Burdick GW. *Phys. Rev. B.*, 2005; **71**:045116.
30. Kaminskii, Alexander A. "Laser Crystals- Their Physics and properties", Springer-Verlag, Berlin, 1979 pp. 20-40.
31. Gill D S, Anderson AA, Eason RW, Warburton TJ, Shepherd DP. *Appl. Phys. Lett.*, 1996; **69**:10-12.
32. Lee JR, Baker HJ, Friel GJ, Hilton GJ, Hall DR. *Opt. Lett.*, 2002; **27**:524-525.